Letter

Streamer formation processes trigger intense x-ray and high-frequency radio emissions in a high-voltage discharge

E. V. Parkevich,[1] K. V. Shpakov,[1] I. S. Baidin,[1] A. A. Rodionov,[1] A. I. Khirianova,[1] T. F. Khirianov,[1] Ya. K. Bolotov,[2,1,*] M. A. Medvedev,[1] V. A. Ryabov,[1] Yu. K. Kurilenkov,[3] and A. V. Oginov[1]

[1]*P. N. Lebedev Physical Institute of the Russian Academy of Sciences, 53 Leninskiy Prospekt, Moscow 119991, Russia*

[2]*Moscow Institute of Physics and Technology, Institutskiy Pereulok 9, Dolgoprudny, Moscow Region 141700, Russia*

[3]*Joint Institute for High Temperatures, Russian Academy of Sciences, Izhorskaya Street 13/2, Moscow 125412, Russia*

(Received 1 March 2022; accepted 6 April 2022; published 2 May 2022)

For a laboratory discharge initiated in a long air gap by a microsecond megavolt pulse, we simultaneously register wideband high-frequency microwave and hard-x-ray emissions and thoroughly analyze the temporal relationship of the emissions depending on the discharge evolution. The temporal structure of microwave radiation is found to consist of numerous short intense bursts with high-frequency components. We directly show that x-ray and microwave emissions can appear almost synchronously in the discharge but only when a complex net of countless plasma channels forms and spans the entire discharge gap. The channel formation is closely related to the intense development of multiple streamers.

DOI: 10.1103/PhysRevE.105.L053201

I. INTRODUCTION

The origin of the intense microwave and x-ray emissions during the development of laboratory and atmospheric discharges is still poorly understood while being highly important in advancing nuclear physics, astrophysics, and gas discharge physics [1–6]. The modern studies associate the sources of high-energy and microwave emissions with local areas wherein the head-on collisions of counterstreamers occur [7]. Upon collision, the counterstreamers are assumed to produce a region with enhanced electric field, where electrons can be accelerated to high energies, as well as trigger the microwave emission having frequencies above 1 GHz due to very rapid current variations [8,9]. This issue, however, is still the subject of discussion. Theoretical investigations indicate that the head-on collision of counterstreamers collapses during a time period much shorter than 1 ns, thereby significant x-ray emissions are unlikely to be produced [10–12]. On the contrary, the results of [13] pointed to the existence of potential or ionization waves propagating along the streamer channels from the zone of the streamer collision. Such waves are capable of increasing the conductivity of the streamer channels and producing electric fields in the counterregion large enough to accelerate electrons to relativistic energies. Recently, in addition to the bremsstrahlung of high-energy runaway electrons [14], a synchrotron radiation mechanism was proposed in [15]. According to this mechanism, x-ray, γ-ray, and microwave emissions can be generated due to fast electromagnetic surface waves moving at a relativistic velocity along a zigzag path of the discharge channel. Importantly, both proposed mechanisms require extended plasma channels that would guide electromagnetic waves. Thus, a certain correlation between the appearance of x-ray and microwave emissions during the discharge development should exist, being driven by the intense streamer formation and collision processes.

In this paper we investigate the development of a laboratory discharge initiated in a long air gap by a microsecond megavolt pulse. The discharge formation is accompanied by x-ray and high-frequency radio emissions which we register in the experiments together with the short-exposure images of the discharge glow. Our findings directly show that the intense development of numerous streamers in the entire discharge gap triggers the generation of the x-ray and microwave emissions.

II. EXPERIMENTAL SETUP

The setup (Fig. 1) employed in the study involves a high-voltage generator [16] which provides a 1-MV voltage pulse (negative polarity) with a duration of approximately 1 μs and a rise time of about several hundred nanoseconds. The pulse is supplied to an open gap with a length of 50 cm. The experiments are carried out in air at normal conditions. The discharge gap is formed by a "needle-inside-cone"-type cathode and a hemispherical wire mesh anode. The discharge voltage is controlled by using the capacitive-resistive voltage divider, with its temporal resolution being better than several nanoseconds.

The x rays from the discharge are registered by two scintillation detectors (SD1 and SD2) placed near the discharge gap as shown in Fig. 1. The detectors are sensitive photomultiplier tubes (1000–5000 A/lm) coupled with fast scintillators [*p*-terphenyl+1,4-bis(5phenyloxazol-2-yl)benzene] and have a temporal resolution of about several nanoseconds. The scintillator properties provide an extremely short delay (less than 100 ps) between the instants an x-ray quantum (with a characteristic energy much less than 1 MeV) is absorbed inside the scintillator and the scintillator substance starts to glow. The detector SD1 has a high aperture and sensitivity and is

*bolotov.yak@phystech.edu

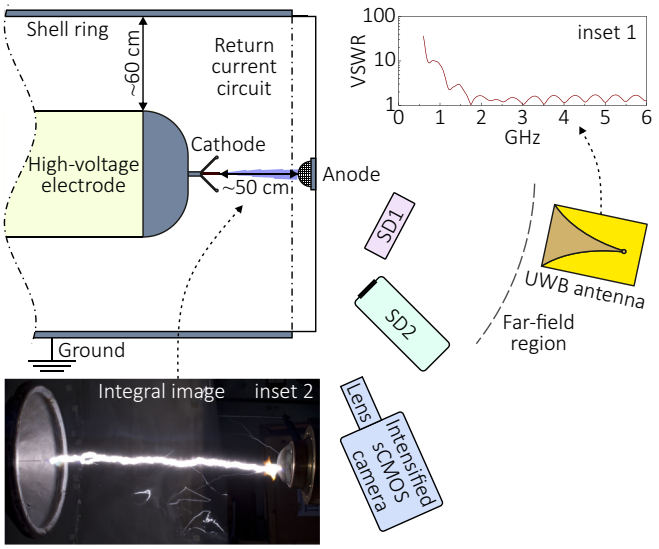

FIG. 1. Schematic representation of the experimental setup. Inset 1 presents the simulated frequency characteristic of an ultrawideband antenna. Inset 2 shows the integral image of the discharge in the gap

used to register x rays in a wide energy range. This detector is covered with a 10-μm aluminum foil additionally shielded with a light-tight paper and has a low threshold energy ($E_\nu \sim$ 20 keV). The detector SD2 is covered with a 1-mm-thick lead filter. In terms of x-ray absorption [17], such a filter has a characteristic threshold energy $E_\nu \sim 100$ keV. All the detectors are precalibrated following the procedure described in [16]. The signals from the x-ray detectors are registered by digital oscilloscopes (1 GHz, 5 GSa/s).

An ultrawideband antenna with an expanding coplanar gap (Vivaldi-type antenna [18]) is placed at a 3 m distance (in the Fraunhofer zone) from the discharge gap to register high-frequency radio emissions. The antenna is vertically polarized and is installed on dielectric tripods. A voltage standing wave ratio (VSWR) of the antenna falls within 1–2 at frequencies of 1–10 GHz and increases sharply in a low-frequency range (less than 1 GHz; see inset 1 of Fig. 1). The antenna signals are recorded by a LeCroy WM8620A oscilloscope (6 GHz, 20 GSa/s). The antenna reliably detects microwave emissions having frequencies within approximately 1–6 GHz.

When registering various electromagnetic emissions, we image the discharge morphology by employing a scientific complementary metal-oxide-semiconductor (sCMOS) gated intensified camera (PCO dicam C1) coupled with a Canon EF 85-mm $f/1.8$ objective. The camera has a multiple-alkali-metal photocathode (S20) and an output phosphor window (P46) and is covered with a bandpass optical filter (300–400 nm). With the camera gate being 55–60 ns, the discharge is imaged at an angle of approximately 60°–70° with respect to the gap axis (see the view of the discharge gap in inset 2 of Fig. 1).

III. RESULTS

Figure 2 presents the chronology of the discharge development. The discharge images (frames 1–6 with a color scale) are recorded in independent shots within different time periods (marked in Fig. 3) of the discharge development with a short exposure time. Notably, an extended horizontal black line, which manifests in each frame, is associated with a structure element of the return current circuit that blocks a part of

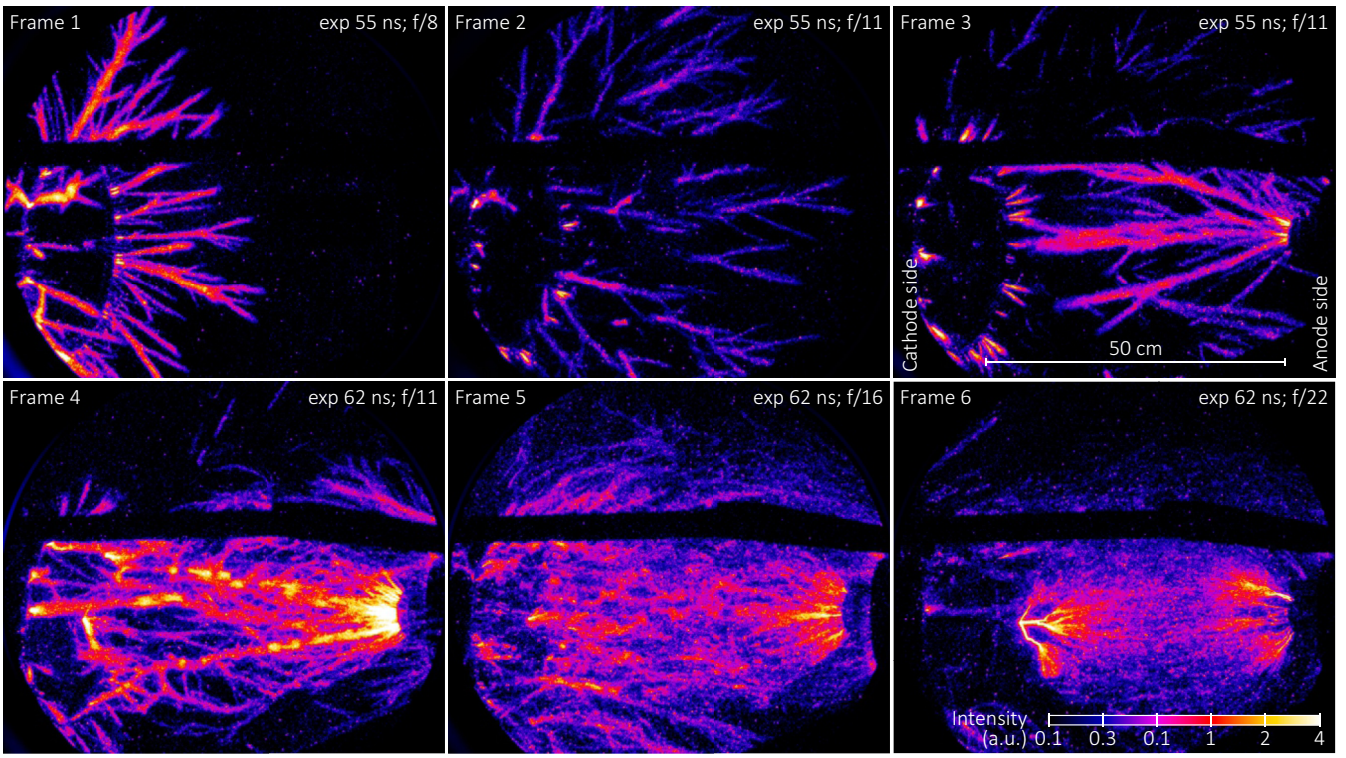

FIG. 2. Discharge images (frames 1–6) obtained in independent shots within different time periods of the discharge development.

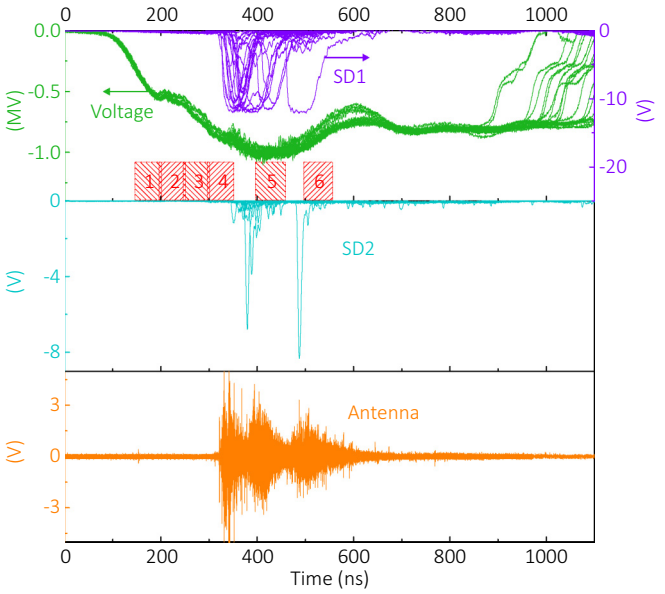

FIG. 3. Superimposed voltage waveforms and x-ray and microwave signals obtained in many discharge events. Digits 1–6 in the top panel indicate the time periods corresponding to the exposure of each frame 1–6 in Fig. 2.

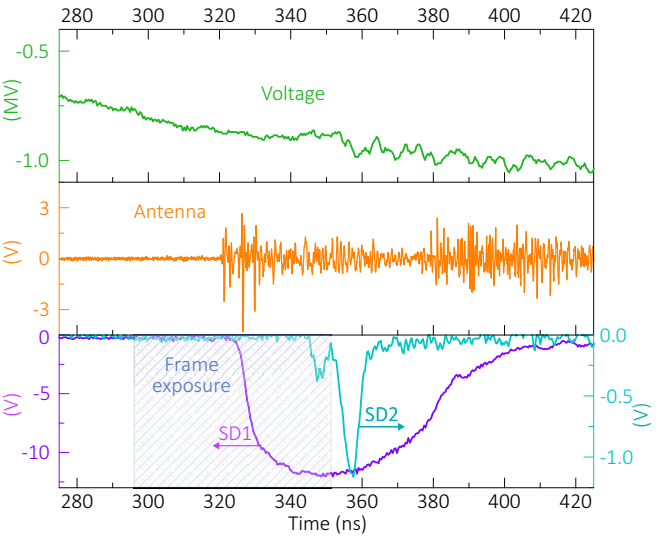

FIG. 4. Voltage waveform and x-ray and microwave signals obtained in a single discharge event corresponding to frame 4 in Fig. 2. The signals are shown for the time period corresponding to the frame exposure.

the discharge glow, entailing a shadow effect. Figure 3 shows superimposed voltage waveforms as well as x-ray and microwave signals obtained in 20 discharge events. The horizontal arrows in the top panel of Fig. 3 point to the corresponding scales of the voltage and x-ray signals. When imaging the discharge, we find that each discharge structure in frames 1–6 is characteristic of a particular time period of the discharge evolution. The good repeatability of the discharge development in time and space from shot to shot is stipulated by the stable temporal characteristics of the employed high-voltage generator (all voltage waveforms reveal similar behavior) and the unchanged key conditions of the experiment.

Once the high-voltage pulse is applied to the gap, the formation of an initial corona starts around the cathode cone edge and at the cathode needle (see frame 1 in Fig. 2). The corona develops and gives rise to many thin streamers propagating from the cathode with an average velocity of the order of 10^8 cm/s (see frame 2 in Fig. 2). The streamers propagate in a wide solid angle and form a complex net of bright plasma channels that are branched in some areas. The streamer heads turn out to be at long distances from the cathode corona, which is well resolved against the propagating streamers in frame 2. With the employed exposure time, the glowing streamer tails seem to be extended, although this effect is probably due to blurring of the moving streamer heads during the exposure [19]. When a part of propagating streamers come close to the anode surface (see frame 3 in Fig. 2) we detect very fast development of streamers originating at the anode surface; these streamers propagate much faster (greater than 10^9 cm/s) than the anode-directed ones.

Statistics show that the discharge stages, during which we register the cathode corona (frame 1), the propagating anode-directed streamers (frame 2), and the streamers quickly developing from the anode (frame 3), are not accompanied by either x-ray or microwave emissions. This is clearly seen in the superimposed signals in Fig. 3. The x-ray and microwave emissions appear only some time (approximately 10 ns) after the fast origination of the streamers at the anode. The x-ray generation starts synchronously with the microwave emission or later, but never before. The appearance of microwave or x-ray emissions always falls within the discharge stage when a complex net of plasma channels forms in the entire discharge gap. As an example, let us consider a single discharge event corresponding to frame 4 in Fig. 2. The obtained voltage, microwave, and x-ray signals are shown in Fig. 4. The horizontal arrows in the bottom panel of Fig. 4 point to the corresponding scales of the x-ray signals. Also in the bottom panel, the time period (62 ns) is marked, during which the discharge glow is registered. Here the onsets of the intense x-ray and microwave emissions fall within the frame exposure time.

Frame 4 shows countless bright plasma channels covering a large zone of the discharge gap from the cathode cone edge to the anode surface. Many channels have a beadlike structure and stochastically wander in space as well as branch. Such discharge morphology is characteristic of extended streamer and corona discharges [19–22]. By taking into account the differences in the discharge structure in frames 3 and 4 in Fig. 2, one can assume that, during a time period of about 10 ns, the rate of the streamer multiplication sharply increases in the entire discharge gap. Streamers originate at the surface of both electrodes and probably in the bulk of the discharge gap. For instance, secondary streamers can develop in local discharge zones corresponding to the branching points of primary anode- and cathode-directed streamers [20]. The plasma system in frame 4 is supposed to be characterized also by multiple head-on collisions of counterstreamers.

The generation of x-ray and microwave radiation most often starts with an increase in the discharge voltage from 0.8 to 1 MV (see Figs. 3 and 4). The x-ray emission is

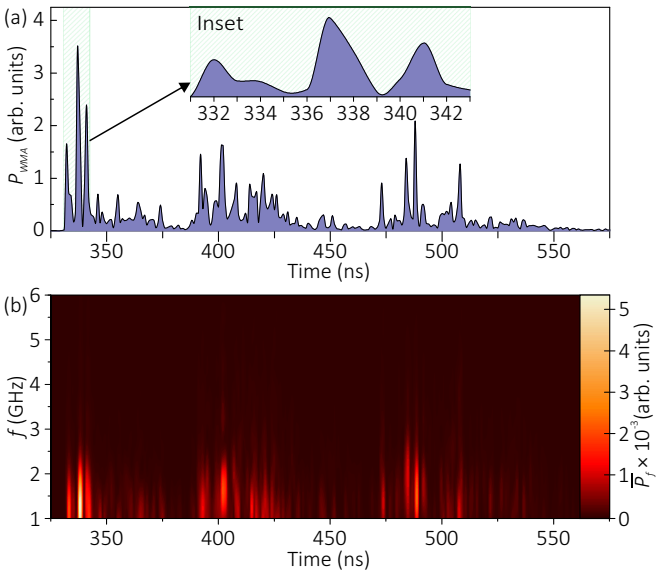

FIG. 5. (a) Weighted moving average $P_{\mathrm{WMA}}(t)$ (over 1 ns) of instantaneous power calculated for the microwave signal in Fig. 4 within 325–550 ns. (b) Map illustrating the evolution of the microwave spectrum in the frequency range of 1–6 GHz. The map intensity characterizes the values of the average instantaneous power $\overline{P}_f(t)$ of the analyzed microwave signal in the time and frequency domain (t, f).

characterized by photons with energies probably no higher than a few hundred keV. In contrast to the detector SD2 ($E_\nu \sim 100$ keV), the sensitive detector SD1 ($E_\nu \sim 20$ keV) registers x rays in each discharge event. Therefore, in our case, the majority of high-energy photons have energies no higher than several tens of keV. Almost all detected x-ray flashes fall within the discharge stage, during which the intense development of bright plasma channels in the entire discharge gap occurs (see frames 4 and 5 in Fig. 2). The x-ray flashes are also detected in the late discharge stage accompanied by the formation of bright leader channels originating from the cathode needle and the anode surface (see frame 6 in Fig. 2). Herein multiple less bright plasma channels closing the heads of the opposite leader channels can be distinguished. As the oppositely directed leaders develop and approach each other, the power of the microwave radiation gradually decreases and the x-ray generation vanishes.

The temporal structure of the microwave signals turns out to be interesting. Let us consider this feature on the example of a single discharge event discussed above. Figure 5(a) demonstrates the linearly weighted moving average $P_{\mathrm{WMA}}(t)$ of instantaneous power obtained for the microwave signal in Fig. 4 within 325–550 ns. The curve $P_{\mathrm{WMA}}(t)$ is iteratively calculated over 1 ns with a step of 50 ps (with the energy conservation taken into account) and illustrates the trend in the signal power over time. Figure 5(b) presents the map illustrating the evolution of the microwave spectrum in the frequency range of 1–6 GHz. The map intensity characterizes the values of the averaged instantaneous power $\overline{P}_f$ of the microwave signal in the time and frequency domain (t, f). The techniques used for obtaining the moving average and microwave spectrum map are described in detail in the Supplemental Material [23]. It can be seen that the high-frequency radio emission is characterized by multiple single bursts concentrated within three key time intervals: ∼325–390 ns, ∼390–450 ns, and ∼470–550 ns. The first time interval contains the most intense microwave bursts. Bursts follow each other with a time step of a few nanoseconds, with the duration of most single bursts being about 1 ns. This is clearly seen in the inset of Fig. 5(a). The first intense bursts in Fig. 5(a) fall within the time interval coinciding with the start of the x-ray generation (see Fig. 4) and the appearance of a complex net of plasma channels in the gap (see frame 4 in Fig. 2). The spectrum of the intense microwave bursts is characterized by the frequencies in the range of 1–3 GHz. The highest values of the spectral power of single bursts are reached at 1–2 GHz. With a typical duration of the intense microwave bursts being about 1 ns, the bursts themselves contain higher-frequency components of the original signal, in some cases, up to 4–5 GHz. Thus, the high-frequency part of the microwave emission is almost completely concentrated inside single intense bursts.

IV. DISCUSSION

Our findings show that the appearance of the intense x-ray and high-frequency radio emissions is closely related with the formation of multiple streamers producing a complex net of plasma channels across the entire discharge gap. We assume that the multiple streamer formation triggers more complex wave subprocesses in the current-carrying plasma channels between the cathode and anode. The channels with moderate electron densities (e.g., of the order of 10^{10}–10^{13} cm^{-3}, which is typical of the streamer channels [24]) can act as single plasma waveguides along which sets of surface and bulk electromagnetic waves can propagate (at almost the speed of light in vacuum) [25]. Such waves can also emit microwave radiation, with their appearance being driven by, e.g., the head-on collisions of counterstreamers. By enhancing the local electric field, the wave fronts propagating along the channels can also lead to electron acceleration and, under certain conditions, this acceleration can be of a resonant character [25]. The proposed hypothesis and obtained results correlate with both the bremsstrahlung of high-energy runaway electrons and the synchrotron mechanism of the x-ray and microwave generation discussed in [13,15]. These mechanisms can be universal for numerous discharge systems wherein runaway electron beams, x rays, and microwave flashes are observed [20,26–32]; however, it cannot be proved without direct correlation studies of the discharge zones producing microwave and x-ray emissions. Nevertheless, we consider the described concept to be promising and requiring rigorous investigation since the intense x-ray and microwave generation fundamentally occurs within the discharge stage during which a complex net of plasma channels is formed and spans the entire discharge gap.

ACKNOWLEDGMENTS

We would like to thank A. V. Gurevich for stimulating the studies of the physics of lightning and runaway breakdown mechanisms. The study was supported by the Russian Foundation for Basic Research through Grant No. 20-08-01156.

[1] A. V. Agafonov, A. V. Bagulya, O. D. Dalkarov, M. A. Negodaev, A. V. Oginov, A. S. Rusetskiy, V. A. Ryabov, and K. V. Shpakov, Observation of Neutron Bursts Produced by Laboratory High-Voltage Atmospheric Discharge, Phys. Rev. Lett. **111**, 115003 (2013).

[2] T. Enoto, Y. Wada, Y. Furuta, K. Nakazawa, T. Yuasa, K. Okuda, K. Makishima, M. Sato, Y. Sato, T. Nakano *et al.*, Photonuclear reactions triggered by lightning discharge, Nature (London) **551**, 481 (2017).

[3] Y. Wada, T. Enoto, K. Nakazawa, Y. Furuta, T. Yuasa, Y. Nakamura, T. Morimoto, T. Matsumoto, K. Makishima, and H. Tsuchiya, Downward Terrestrial Gamma-Ray Flash Observed in a Winter Thunderstorm, Phys. Rev. Lett. **123**, 061103 (2019).

[4] B. M. Hare, O. Scholten, J. Dwyer, T. N. G. Trinh, S. Buitink, S. Ter Veen, A. Bonardi, A. Corstanje, H. Falcke, J. R. Hörandel *et al.*, Needle-like structures discovered on positively charged lightning branches, Nature (London) **568**, 360 (2019).

[5] B. M. Hare, O. Scholten, J. Dwyer, U. Ebert, S. Nijdam, A. Bonardi, S. Buitink, A. Corstanje, H. Falcke, T. Huege, J. R. Hörandel, G. K. Krampah, P. Mitra, K. Mulrey, B. Neijzen, A. Nelles, H. Pandya, J. P. Rachen, L. Rossetto, T. N. G. Trinh *et al.*, Radio Emission Reveals Inner Meter-Scale Structure of Negative Lightning Leader Steps, Phys. Rev. Lett. **124**, 105101 (2020).

[6] O. Scholten, B. M. Hare, J. Dwyer, N. Liu, C. Sterpka, I. Kolmašová, O. Santolik, R. Lan, L. Uhlíř, S. Buitink, T. Huege, A. Nelles, and S. ter Veen, Interferometric imaging of intensely radiating negative leaders, Phys. Rev. D **105**, 062007 (2022).

[7] J. R. Dwyer and M. A. Uman, The physics of lightning, Phys. Rep. **534**, 147 (2014).

[8] F. Shi, N. Liu, J. R. Dwyer, and K. M. A. Ihaddadene, VHF and UHF electromagnetic radiation produced by streamers in lightning, Geophys. Res. Lett. **46**, 443 (2019).

[9] J. Koile, N. Liu, and J. Dwyer, Radio frequency emissions from streamer collisions in subbreakdown fields, Geophys. Res. Lett. **48**, e2021GL096214 (2021).

[10] M. A. Ihaddadene and S. Celestin, Increase of the electric field in head-on collisions between negative and positive streamers, Geophys. Res. Lett. **42**, 5644 (2015).

[11] C. Köhn, O. Chanrion, and T. Neubert, Electron acceleration during streamer collisions in air, Geophys. Res. Lett. **44**, 2604 (2017).

[12] L. Babich and E. Bochkov, Numerical simulation of electric field enhancement at the contact of positive and negative streamers in relation to the problem of runaway electron generation in lightning and in long laboratory sparks, J. Phys. D **50**, 455202 (2017).

[13] V. Cooray, G. Cooray, M. Rubinstein, and F. Rachidi, Ionization waves enhance the production of X-rays during streamer collisions, Atmosphere **12**, 1101 (2021).

[14] R. A. Roussel-Dupre, A. V. Gurevich, T. Tunnell, and G. M. Milikh, Kinetic theory of runaway air breakdown, Phys. Rev. E **49**, 2257 (1994).

[15] N. I. Petrov, Synchrotron mechanism of X-ray and gamma-ray emissions in lightning and spark discharges, Sci. Rep. **11**, 19824 (2021).

[16] A. V. Agafonov, V. A. Bogachenkov, A. P. Chubenko, A. V. Oginov, A. A. Rodionov, A. S. Rusetskiy, V. A. Ryabov, A. L. Shepetov, and K. V. Shpakov, Observation of hard radiations in a laboratory atmospheric high-voltage discharge, J. Phys. D **50**, 165202 (2017).

[17] I. K. Kikoin, *Tables of Physical Values* (Atomizdat, Moscow, 1976) (in Russian).

[18] M. Pasternak, *2018 14th International Conference on Advanced Trends in Radioelecrtronics, Telecommunications and Computer Engineering (TCSET)* (IEEE, Piscataway, 2018), pp. 624–627.

[19] E. van Veldhuizen, P. Kemps, and W. Rutgers, Streamer branching in a short gap: The influence of the power supply, IEEE Trans. Plasma Sci. **30**, 162 (2002).

[20] P. O. Kochkin, A. P. J. van Deursen, and U. Ebert, Experimental study of the spatio-temporal development of metre-scale negative discharge in air, J. Phys. D **47**, 145203 (2014).

[21] P. Kochkin, C. Köhn, U. Ebert, and L. van Deursen, Analyzing x-ray emissions from meter-scale negative discharges in ambient air, Plasma Sources Sci. Technol. **25**, 044002 (2016).

[22] R. Ono and T. Oda, Formation and structure of primary and secondary streamers in positive pulsed corona discharge—Effect of oxygen concentration and applied voltage, J. Phys. D **36**, 1952 (2003).

[23] See Supplemental Material at http://link.aps.org/supplemental/10.1103/PhysRevE.105.L053201 for more details.

[24] S. Nijdam, J. Teunissen, and U. Ebert, The physics of streamer discharge phenomena, Plasma Sources Sci. Technol. **29**, 103001 (2020).

[25] M. V. Kuzelev and A. A. Rukhadze, Waves in inhomogeneous plasmas and liquid and gas flows. Analogies between electro- and gas-dynamic phenomena, Phys. Usp. **61**, 748 (2018).

[26] T. Shao, V. Tarasenko, C. Zhang, D. Rybka, I. Kostyrya, A. Kozyrev, P. Yan, and V. Y. Kozhevnikov, Runaway electrons and x-rays from a corona discharge in atmospheric pressure air, New J. Phys. **13**, 113035 (2011).

[27] V. Tarasenko, Runaway electrons in diffuse gas discharges, Plasma Sources Sci. Technol. **29**, 034001 (2020).

[28] M. Rahman, P. Hettiarachchi, V. Cooray, J. Dwyer, V. Rakov, and H. K. Rassoul, Observations of x-rays from laboratory sparks in air at atmospheric pressure under negative switching impulse voltages, Atmosphere **10**, 169 (2019).

[29] C. L. da Silva, R. M. Millan, D. G. McGaw, C. T. Yu, A. S. Putter, J. LaBelle, and J. Dwyer, Laboratory measurements of x-ray emissions from centimeter-long streamer corona discharges, Geophys. Res. Lett. **44**, 11 (2017).

[30] J. Montanyà, F. Fabró, V. March, O. van der Velde, G. Solà, D. Romero, and O. Argemí, X-rays and microwave rf power from high voltage laboratory sparks, J. Atmos. Sol. Terr. Phys. **136**, 94 (2015).

[31] M. Gushchin, S. Korobkov, I. Y. Zudin, A. Nikolenko, P. Mikryukov, V. Syssoev, D. Sukharevsky, A. Orlov, M. Y. Naumova, Y. A. Kuznetsov *et al.*, Nanosecond electromagnetic pulses generated by electric discharges: Observation with clouds of charged water droplets and implications for lightning, Geophys. Res. Lett. **48**, e2020GL092108 (2021).

[32] N. Liu, O. Scholten, B. M. Hare, J. R. Dwyer, C. F. Sterpka, I. Kolmašová, and O. Santolík, LOFAR observations of lightning initial breakdown pulses, Geophys. Res. Lett. **49**, e2022GL098073.